Eur. Phys. J. B **48**, 379–383 (2005)
DOI: 10.1140/epjb/e2005-00415-9

THE EUROPEAN PHYSICAL JOURNAL B

Buckling of a compressed elastic membrane: a simple model

P. Peyla[a]

Laboratoire de Spectrométrie Physique, UJF - CNRS, 38402 Saint-Martin d'Hères, Cedex, France

Received 12 August 2005
Published online 23 December 2005 –

Abstract. The buckling of a folded membrane submitted to a bi-axial compression is studied in the framework of the continuum non-linear elasticity theory. We show that the formation of the fold patterning can be quantitatively well described with a simple non-linear model. As a matter of fact, with this model, we recover the experimental phase diagram of a secondary buckling instability with a very good precision. In addition, depending on the anisotropy of the applied compressive stress, we find that the buckling coarsening dynamics can be described as a 1D spinodal decomposition (for a uni-axial stress) or as a 2D XY model (for an isotropic bi-axial stress) with an irrotational non-scalar order parameter. For an isotropic bi-axial stress, we indeed recover the famous coarsening exponent: $n = 1/4$. This exponent has to be confirmed experimentally.

PACS. 46.32.+x Static buckling and instability – 05.45.-a Nonlinear dynamics and nonlinear dynamical systems

1 Introduction

In very different fields of physics, problems involving mechanics of thin elastic sheet like tethered membranes [1], biological cell membranes [2], solid langmuir monolayers [3], atomic sheets [4], thin films [5] and thin plates [6] have attracted a lot of interest in recent years. In this paper, we address the far-from-equilibrium buckling of a thin elastic sheet. This study is carried on in the framework of continuum non-linear elasticity theory. We derive a simplified continuum non-linear kinetic equation that gives stationary solutions reproducing very well the experimentally observed structures of a thin elastic plates [6].

2 The simplified continuum model

We consider a bi-axially compressed thin elastic membrane (or a film) of thickness h parallel to the xOy horizontal plane in its reference state. The film can buckle away from its horizontal plane along the perpendicular direction Oz in order to relax the in-plane compressive stress. We note $\mathbf{u}(u_x, u_y, \zeta)$ the displacement field. For large vertical deflection field $\zeta(x, y)$, the in-plane components of the strain tensor is as follows:

$$u_{\alpha\beta} = \frac{1}{2}\left(\frac{\partial u_\alpha}{\partial x_\beta} + \frac{\partial u_\beta}{\partial x_\alpha}\right) + \frac{1}{2}\frac{\partial \zeta}{\partial x_\alpha}\frac{\partial \zeta}{\partial x_\beta} - \epsilon^*_{\alpha\beta}, \qquad (1)$$

where x_α and x_β represent x or y. The first term is the usual linear elastic strain while the second one is the non-linear contribution of the buckling [7] and the third term is the pre-strain ($\epsilon^*_{\alpha\beta} > 0$ for compression) in the reference state (marked by a star). In the following, we use the general assumption that the modulus of any gradient of the displacement (a dimensionless quantity) must remain small. This assumption allows one to use the Hook's linear law relating the components of the stress tensor σ to the above strain tensor components [7]:

$$\sigma_{\alpha\beta} = \frac{E}{1-\nu^2}\left[(1-\nu)u_{\alpha\beta} + \nu u_{\gamma\gamma}\delta_{\alpha\beta}\right], \qquad (2)$$

(Einstein's convention has been used all along this paper). In the following, the stress $\sigma^*_{\alpha\beta}$ will refer to the applied stress in the reference state. The elastic constants, i.e. the Young's Modulus E and the Poisson's ratio ν both depend on temperature. Thus, a free elastic energy $\mathcal{F}$ of the buckled membrane can be written as [7]:

$$\mathcal{F} = \frac{1}{2}\int dx\, dy\, \left[Df(\zeta) + h\sigma_{\alpha\beta}u_{\alpha\beta}\right], \qquad (3)$$

with

$$f(\zeta) = (\Delta\zeta)^2 + 2(1-\nu)\left[\left(\frac{\partial^2\zeta}{\partial x \partial y}\right)^2 - \frac{\partial^2\zeta}{\partial x^2}\frac{\partial^2\zeta}{\partial y^2}\right], \qquad (4)$$

D being the bending coefficient ($D = Eh^3/[12(1-\nu^2)]$). The first term in equation (3) is usually called the linear

[a] e-mail: philippe.peyla@ujf-grenoble.fr

bending term while the second one is known as the non-linear membrane term. Now, we study the overdamped dynamics of such a stressed membrane (as if it was immersed in a viscous fluid). We consider a time dependent Ginsburg-Landau gradient flow kinetics [8]:

$$\begin{cases} \frac{1}{\Gamma}\frac{\partial\zeta}{\partial t} = -\frac{\delta\mathcal{F}}{\delta\zeta} = -D\Delta^2\zeta + h\frac{\partial}{\partial x_\beta}(\sigma_{\alpha\beta}\frac{\partial\zeta}{\partial x_\alpha}) \\ \frac{1}{\Gamma'}\frac{\partial u_\alpha}{\partial t} = -\frac{\delta\mathcal{F}}{\delta u_\alpha} = h\frac{\partial\sigma_{\alpha\beta}}{\partial x_\beta}, \end{cases} \quad (5)$$

the x, y, z-components of the displacement field $\mathbf{u}$ being the three order parameters, Γ and Γ' are kinetic coefficients. This can also be viewed for a polymer membrane as an overdamped Rouse dynamics [9] while we neglect inertia and the long-range effect of hydrodynamic backflow on the membrane. At stationarity, equations (5) represent the famous Föppl von Karmann (FvK) equations that describe the out-of-plane buckling (Oz-direction) of an elastic plate of thickness h much smaller than the typical lengthscale λ along the horizontal directions (xOy). Despite their complicated form (4th order of derivation and highly non-linear character) the remarkable property of FvK equations is that they are variational. Hence, stationary solutions, even in a strong non-linear regime, are physically relevant [10].

In order to simplify the problem, we assume that the in-plane components of the displacement (u_x, u_y) are indeed negligible in comparison to the large out-of-plane displacement ζ, we set $u_x = u_y = 0$. This assumption has also been considered by Ortiz et al. [11] to describe large blister stationary shapes in the case of thin film delamination. With this approximation, the equation describing the buckling dynamics involves only a single order parameter: ζ.

Thus, by varying $\mathcal{F}$, we get (without any applied shear stress, i.e. $\epsilon_{xy} = 0$):

$$\frac{\partial\zeta}{\partial t} = -A\left(\frac{h^2}{6}\Delta^2\zeta - \frac{\partial}{\partial x}\left[\phi_x(\zeta)\frac{\partial\zeta}{\partial x}\right] - \frac{\partial}{\partial y}\left[\phi_y(\zeta)\frac{\partial\zeta}{\partial y}\right]\right), \quad (6)$$

with

$$\begin{cases} \phi_x(\zeta) = |\nabla\zeta|^2 - 2\left(\epsilon^*_{xx} + \nu\epsilon^*_{yy}\right) \\ \phi_y(\zeta) = |\nabla\zeta|^2 - 2\left(\epsilon^*_{yy} + \nu\epsilon^*_{xx}\right), \end{cases} \quad (7)$$

and with $A = Eh/[2(1-\nu^2]$. The kinetic coefficient has been absorbed in time scale. When the applied bi-axial compression is isotropic ($\epsilon^*_{\alpha\beta} = \epsilon^*\delta_{\alpha\beta}$), equation (6) reads:

$$\frac{\partial\zeta}{\partial t} = -A\left(\frac{h^2}{6}\Delta^2\zeta - \nabla\left\{\left[|\nabla\zeta|^2 - g_0^2\right]\nabla\zeta\right\}\right), \quad (8)$$

where $g_0^2 = 2(1+\nu)\epsilon^*$. The stationary solutions of equation (8) have been studied in several publications [11,12]. When the film thickness is small in comparison with the typical wave length of the folds λ, the bending term ($\Delta^2\zeta$) is generally considered as a singular perturbation. Thus, the minimisation of $\mathcal{F}$ is achieved when $|\nabla\zeta| = g_0$ (Eikonal equation) giving rise to facets. Considering equation (3), it is easy to show that $\mathcal{F}$ contains a double well potential $V(|\nabla\zeta|) = \frac{1}{8}\frac{Eh}{(1-\nu^2)}(|\nabla\zeta|^2 - g_0^2)^2$ leading to a stable equilibrium when the slope is such that $|\nabla\zeta| = \pm g_0$, while flat regions ($\nabla\zeta = 0$) are unstable. The singular perturbation bending term minimizes the number of folds that have a cost in energy. Therefore, it appears that equations (6) and (8) contain the main physical ingredients that lead to the buckling instability of a compressed elastic membrane.

3 Phase diagram for a static buckling

In order to show that equation (6) captures the main features of buckling physics, we consider a single longitudinal fold parallel to the x-direction (Fig. 1a) of a thin plate submitted to an external bi-axial compression. Equation (6) is integrated numerically with periodic boundary conditions along x- and y-axis. A 2D fast Fourier transform is used to compute the spatial derivatives while the non-linear terms are calculated in real space.

Depending on the external applied stress, we calculate that such a fold evolves to give rise to mainly four non-trivial remarkable structures: a longitudinal (L) (Fig. 1b), a bumped (B) (Fig. 1c), a wavy (W) (Fig. 1d) and a flat (F) structure. These results are indeed consistent with experimental results [6]. The experimental phase diagram has been reproduced from [6] in Figure 2a.

Note that we do not obtain the so-called oblique shape (OB) of reference [6] which seems, according to our results, to depend critically on initial conditions. The theoretical phase diagram obtained with our model, is presented in Figure 2b: it reproduces the experimental one (Fig. 2a) with very good precision.

Consistently with experimental results [6], we find that the applied stress should be much bigger than the Euler column stress $\sigma_0 = Eh^2\pi/[12b^2(1-\nu^2)]$ where b is the half width of the column. Note that σ_0 is calculated for an assumed cosine transverse shape which is not the case here since $|\nabla\zeta|$ is a constant except on folds. As a consequence σ_0 is no longer the threshold of the instability (Fig. 2b).

The comparison between our results and experiments validates equation (6), i.e. the assumption that the in-plane components of the displacement can be indeed neglected for such an experiment.

4 The dynamics

As equation (6) predicts very well the stationary structures, we should also check the dynamics for which, according to our knowledges, no measure has been done. In order to address that question, we must make the following remarks. For sake of simplicity, we consider the isotropic case $\epsilon_{\alpha\beta} = \epsilon^*\delta_{\alpha\beta}$. By setting $\mathbf{g} = \nabla\zeta$ and using equation (8), we get the conservative kinetic equation for $\mathbf{g}$:

$$\frac{\partial\mathbf{g}}{\partial t} = -A\nabla^2\left[\frac{h^2}{6}\nabla^2\mathbf{g} - \mathbf{g}\left(\mathbf{g}^2 - g_0^2\right)\right], \quad (9)$$

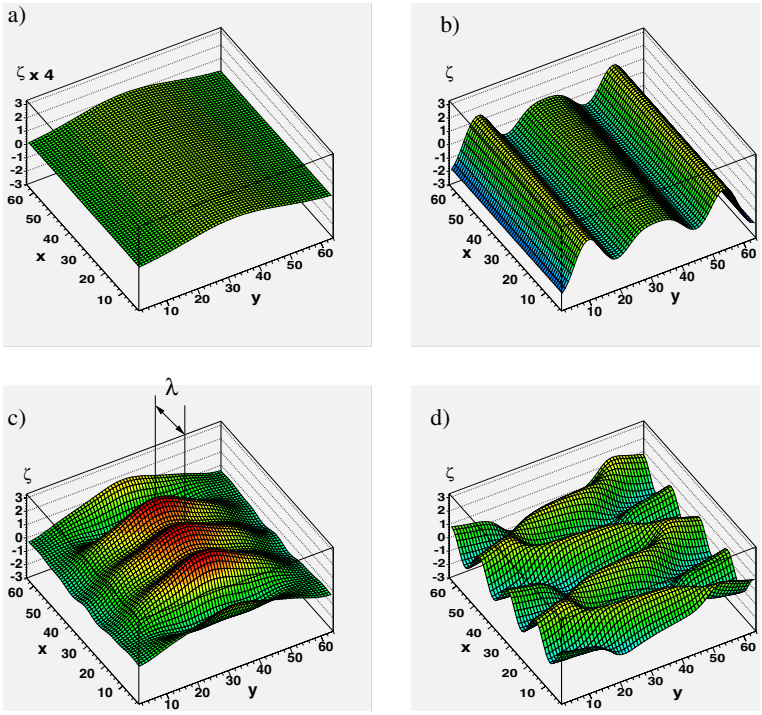

Fig. 1. Different calculated shapes (obtained after $\Gamma t = 8 \times 10^4$) adopted by a fold submitted to a bi-axial compression: (a) initial fold; (b) longitudinal fold (L) ($-\sigma^*_{xx}/\sigma_0 = 3$, $-\sigma_{yy}/\sigma^*_0 = 7$); (c) bump ($B$)($-\sigma^*_{xx}/\sigma_0 = 7$, $-\sigma^*_{yy}/\sigma_0 = 3$); (d) wavy ($W$)($-\sigma^*_{xx}/\sigma_0 = 12$, $-\sigma^*_{yy}/\sigma_0 = 10$). Parameters (see text): $E = 10^{11}\ Pa$, $\nu = 0.3$, $h/b = 1/16$.

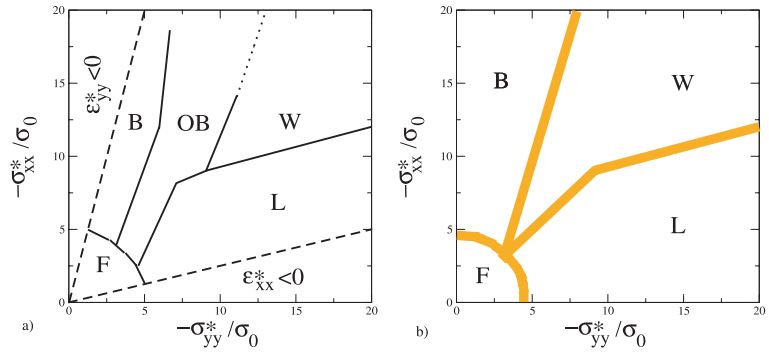

Fig. 2. (a) Experimental phase diagram of a buckled thin plate submitted to a bi-axial compression (Reproduced from Ref. [6]). (F) unbuckled, (L) longitudinal, (B) bumped, (OB) oblique and (W) wavy like configuration; (b) Our theoretical phase diagram. The initial longitudinal fold is parallel to the x-direction. The parameters are the same as the ones in Figure 1. The thickness of the gray lines indicates the uncertainty due to the determination of transition lines between the different domains.

where we have used the fact that $\nabla \times \mathbf{g} = 0$. Note that $\mathbf{g}$ is a vector and equation (9) is the one that describes the 2D XY model [13,14] or the coarsening of a crystal surface during molecular beam epitaxy with slope selection [15]. This equation couples the components of $\mathbf{g}$, this coupling is known to produce a slower growth of domain than the usual Lifshitz-Slyozov and Wagner dynamics where $\lambda(t) \sim t^n$ with $n = 1/3$ [16]: for equation (9) Siegert et al. [15] give $n = 1/4$. It is known [16,14] that usual theories of phase ordering cannot be applied to the 2D XY model due to the long range correlations between vortices. But, as mentioned by Siegert et al. [15], there is an important difference between the slope $\mathbf{g}$ and the order parameter of an XY model: the slope must obey the constraint $\nabla \times \mathbf{g} = 0$ which is suspected to slow down the dynamics.

Now, if we only consider a uniaxial compression: for example $\epsilon^*_{yy} = \epsilon^*$ and $\epsilon^*_{xx} = 0$ and a 1D buckling $\zeta(x)$, we get the 1D equivalent of equation (9) which is the 1D Kahn-Hilliard equation, also well known as model B in the Hohenberg and Halperin classification [17]. This equation is currently used to describe the spinodal decomposition in alloys. Langer [18] has shown that in absence of noise, the rate at which the structure coarsens is a logarithmic function of time. The absence of noise in equation (9) indicates that we are working at temperature $T = 0$. It has been shown by Bray [19] that when the characteristic scale λ of the domain pattern is large compared with

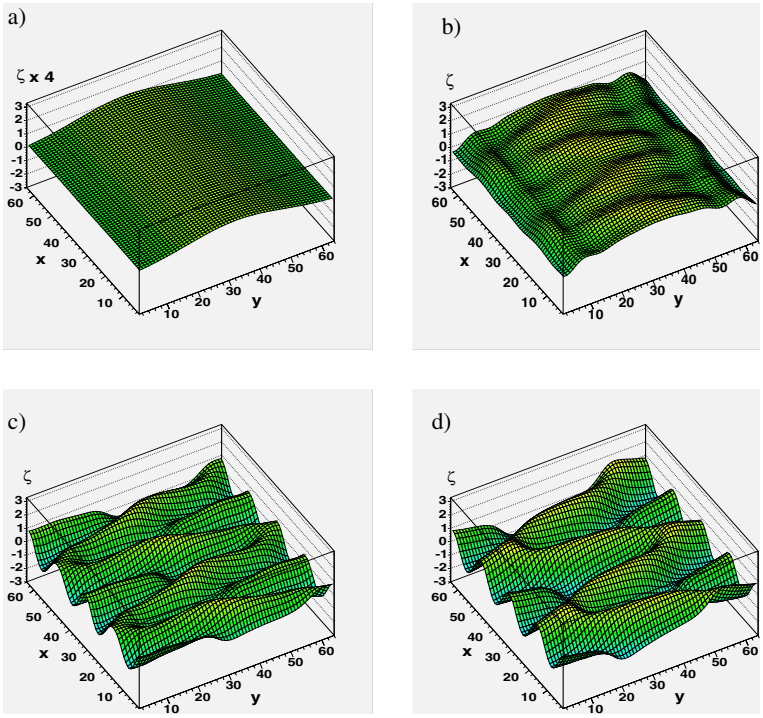

Fig. 3. Time evolution of an initially longitudinal fold (parallel to $0x$) submitted to a bi-axial compression with $-\sigma^*_{xx}/\sigma_0 = 12$ and $-\sigma^*_{yy}/\sigma_0 = 10$. (a) $t = 0$; (b) $t = 1000$; (c) $t = 18\,000$; (d) $t = 80\,000$. The other parameters are the same as the ones in Figure 1.

the domain wall thickness the system behaves as if it were at $T = 0$, the temperature dependence entering through T-dependent model parameters (which is the case here for the elastic constants).

For both limits (uniaxial stress and isotropic biaxial stress), we can consider the buckled structure as domains of constant slope $\pm g_0$ separated by walls (the folds). Therefore, for these two limits the coarsening dynamics of equation (8) should be identical to the one of equation (9).

We define $\alpha = \sigma^*_{xx}/\sigma^*_{yy}$ that measures the anisotropy of the applied stress on the membrane. We start with the initial structure represented in Figure 3a, and we calculate the average thickness $w(t) = \langle \zeta^2(r,t) \rangle^{1/2}$ for different values of α ranking between 0 (uniaxial transverse stress σ_{yy}) and 1 (isotropic bi-axial stress $\sigma^*_{xx} = \sigma^*_{yy}$). The effective time t varies from 0 to 9×10^4. For both limit ($1D$ and isotropic), we calculate the first zero of the correlation functions $C_\zeta(r,t) = \langle \zeta(r+s,t)\zeta(r,t) \rangle$ and $C_g(r,t) = \langle \mathbf{g}(r+s,t)\mathbf{g}(r,t) \rangle$.

The inset of Figure 4, shows how the exponent n varies when the stress σ_{xx} varies at fixed $\sigma_{yy} = 15\,\sigma_0$, $(0 \leq \alpha \leq 1)$. Note that for the anisotropic case, the values of n extracted from $C_\zeta(r)$ and $C_g(r)$ are not really exploitable since the coarsening dynamics depends on at least two length scales with different time dependence [20]. In that case standard scaling assumptions are invalid. However, $w(t) \sim t^n$ presents a notable difference depending on which domain (L or W) of the phase diagram is explored. The range $0 \leq \alpha \leq 0.65 \pm 0.05$ corresponds to a longitudinal pattern (L) (see Fig. 2) [21]. In that case, the dynamics is extremely slow consistently

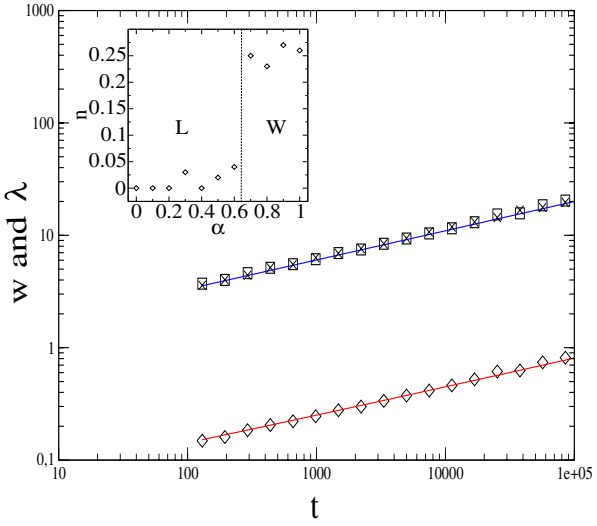

Fig. 4. Isotropic applied stress ($\epsilon* = 0.01$). Variations of $w(t)$ (diamonds) and $\lambda(t)$ [obtained with $C_\zeta(r)$(crosses) and with $C_g(r)$ (squares)]. Lines are guides for the eyes. We find $n = 0.26 \pm 0.02$. Points for which $t < 100$ are not plotted. Inset: the coarsening exponent n as a function of the anisotropy α of the applied stress. Diamonds are obtained from $w(t)$ (see text). The stress σ^*_{yy} is maintained at $\sigma^*_{yy} = 15\,\sigma_0$ while σ^*_{xx} varies from 0 to $\sigma^*_{xx} = 15\,\sigma_0$.

with a 1D spinodal decomposition without noise [18]. The dynamics of coarsening speeds up when we cross the transition line L/W to fall in the domain of the wavy like structures where α is increased toward $\alpha = 1$. For an isotropic applied bi-axial stress (i.e. $\alpha = 1$), we found

$n = 0.26 \pm 0.02$ consistently with [15,22]. Note that due to the anisotropic pre-strain, equation (6) cannot map the Siegert's model [20] exactly.

5 Conclusions

In conclusion, we have shown that in order to describe the buckling of an elastic membrane or a film, the in-plane displacement field can be neglected in the equation of nonlinear elasticity. The stationary buckled structures of a plate submitted to a bi-axial compression observed experimentally as well as their phase diagram are indeed very well reproduced within this approximation. With such an approximation, we have shown that the corresponding dynamical equation maps exactly with the one of the 2D-XY-model with an irrotational order parameter which fixes the coarsening exponent to 0.26 ± 0.02 (roughly 1/4). If such an exponent could be confirmed experimentally, the dynamics of a buckling elastic membrane would not be a new class of dynamical systems but could be considered as a tunable dynamics — by the applied compression- that interpolates two well known asymptotic limits: a 1D spinodal decomposition and a 2D XY model with an irrotational non-scalar order parameter.

Simulations were performed on the parallel cluster *Phynum* of Joseph Fourier University. The author gratefully acknowledges the Centre Jacques Cartier for its financial support.

References

1. M.S. Spector, E. Naranjo, S. Chiruvolu, J.A. Zasadzinshi, Phys. Rev. Lett. **73**, 2867 (1994)
2. G. Lenormand, S. Henon, A. Richet, J. Simeon, F. Gallet, Bio. Phys. J. **81**, 43 (2001)
3. A. Saint-Jalmes, F. Gallet, Eur. Phys. J. B **2**, 489 (1998)
4. A. Incze, A. Pasturel, P. Peyla, Elastic interaction of oxygen atoms on a graphite surface, Phys. Rev. B **66**, 172101 (2002)
5. G. Gioia, M. Ortiz, Adv. in Appl. Mech. **33**, 119 (1997)
6. B. Audoly, B. Roman, A. Pocheau, Eur. Phys. J. B **27**, 7 (2002)
7. L.D. Landau, E. Lifchitz, *Theory of elasticity* (Mir Editions, Moscow, 1991)
8. The variation of $\mathcal{F}$ gives rise to terms involving boundary conditions [7]. These terms cancel out while considering an infinite (the case here) or a clambed membrane
9. M. Doi, S.F. Edwards, *The theory of polymer dynamics*, (Oxford University Press, Oxford, 1986)
10. Y. Pomeau, Phil. Mag. B **78**, 235 (1998)
11. M. Ortiz, G. Gioia, J. Mech. Phys. Solids **42**, 531 (1994)
12. W. Jin, P. Sternberg, J. Math. Phys. **42**, 192 (2001)
13. M. Siegert, M. Rao, Phys. Rev. Lett. **70**, 1956 (1993)
14. A.J. Bray, A.D. Rutenberg, Phys. Rev. E **49**, R27 (1994)
15. M. Siegert, M. Plischke, Phys. Rev. Lett. **73**, 1517 (1994)
16. A.J. Bray, Adv. Phys. **51**, 481 (2002)
17. P.C. Hohenberg, B.I. Halperin, Theory of dynamic critical phenomena, Rev. Mod. Phys. **49**, 435 (1977)
18. J.S. Langer, Ann. Phys. **65**, 53 (1971)
19. A.J. Bray, Phys. Rev. Lett. **62**, 2841 (1989)
20. M. Siegert, Phys. Rev. Lett. **81**, 5481 (1998)
21. Note that our initial state ($t = 0$) is the macroscopic fold represented in Figure 1a and not a random fluctuation as it could be also choosed. This choice is more convenient in order to observe the dynamics of the pattern formation given by the phase diagram (Fig. 2)
22. M. Rost, J. Krug, Phys. Rev. E **55**, 3952 (1997)